Nonlinear Control of Active Magnetic Bearings: A Backstepping Approach

Marcio S. de Queiroz and Darren M. Dawson, *Senior Member, IEEE*

Abstract— **In this paper, we utilize a nonlinear model of a planar rotor disk, active magnetic bearing system to develop a nonlinear controller for the full-order electromechanical system. The controller requires measurement of the rotor position, rotor velocity, and stator current and achieves global exponential rotor position tracking. Simulations are provided to illustrate the performance of the controller.**

I. Introduction

In a typical magnetic bearing application, the magnetic forces, which are applied by sets of stator electromagnets (see Fig. 1), must be adjusted online to ensure that the rotor is accurately positioned; however, the control problem is complicated due to the inherent nonlinearities associated with the electromechanical dynamics (for a review of the evolution of magnetic bearing hardware, the reader is referred to [2]). As pointed out in [11], the use of magnetic bearings in industrial and manufacturing applications will most likely increase due to their ability to suspend high-speed rotating loads with no friction and operate under environmental constraints which prevent the use of lubrication. Since magnetic bearings can be actively controlled, they offer many other potential advantages [12] over conventional bearings such as eliminating vibration through active damping, adjusting the stiffness of the suspending load, or providing an automatic balancing capability. As pointed out in [16], many of the previous active magnetic bearing (AMB) control techniques are based on the linearized electromechanical system. For example, Matsumura *et al.* [11] designed an optimal controller to regulate the rotor position. In [12], Mohamed *et al.* used the Q-parameterization theory to stabilize the rotor position and evaluate noise rejection and robustness to parametric uncertainty. Later, in [13], Mohamed *et al.* illustrated how the Q-parameterization theory could be used to autobalance the rotor of a vertical shaft AMB system. In [1], Beale *et al.* introduced an adaptive forced balancing controller which exhibited negligible effects on the bandwidth and the stability margin. In [16], Smith *et al.* provided a starting point for addressing the possible advantages or disadvantages of nonlinear control techniques for AMB applications. Specifically, Smith *et al.* utilized input–output feedback linearization and sliding mode control techniques to center the rotor in a set of magnetic bearings (see [6] for other work based on input–output feedback linearization).

In the last couple of years, the integrator backstepping (IB) control technique [10] has received a great deal of attention since it provides the framework for attacking many electromechanical control problems similar to AMB applications. One of the main advantages of the IB family of control design tools is the proviso for systematic desirable modifications of the control structure such as compensation for parametric uncertainty or eliminating state measurements (i.e., adaptive IB and observed IB [10]). Fortunately, the structure of the magnetic bearing dynamics facilitates the use of the IB technique. Specifically, the electromechanical system of a magnetic bearing can be subdivided into the mechanical subsystem dynamics, the algebraic force transmission relationship, and the electrical subsystem dynamics. If one utilizes the co-energy method [19] to derive a set of equations for control design purposes, the flux linkage model determines the complexity of the resulting dynamics. That is, at least in principle, standard calculations can be applied to the flux linkage model to complete the description of the electrical subsystem dynamics and the algebraic force transmission relationship. Based on this fact, we use a nonlinear model for a planar rotor disk AMB system to develop a *backstepping*-type controller. That is, we first design a desired force trajectory signal to ensure that the rotor position tracks a desired position trajectory. We then use the structure of the algebraic force transmission relationship to develop a static equation which ensures that the desired force is delivered to the mechanical subsystem. The continuation of the backstepping control design procedure is facilitated by requiring that the desired current trajectory signals be constructed to satisfy this static equation. The desired current trajectory signals are then used as the control objective for the design of voltage input, current tracking controllers for the electrical subsystem dynamics. Finally, a composite Lyapunov function is used to illustrate global exponential rotor position tracking. We then use an example flux linkage model, which was used in the design of the controller presented in [16], to illustrate how the desired current trajectory signals can be constructed[1] to ensure that the desired force is delivered to the mechanical

Manuscript received September 29, 1995; revised January 29, 1996. This work was supported in part by the U.S. National Science Foundation Grants DMI-9457967, DDM-931133269, Department of Energy Contract DE-AC21-92MC29115, the Office of Naval Research Grant URI-3139-YIP01, the Union Camp Corporation, the AT&T Foundation, and the National Research Council-CNPq, Brazil.

The authors are with the Department of Electrical and Computer Engineering, Center for Advanced Manufacturing, Clemson University, Clemson, SC 29634-0915 USA.

Publisher Item Identifier S 1063-6536(96)06628-6.

[1] In the electric motor control field, the procedure of constructing the desired current trajectory signals such that the algebraic *torque* transmission relationship outputs the desired *torque* trajectory signal is often called a commutation strategy.

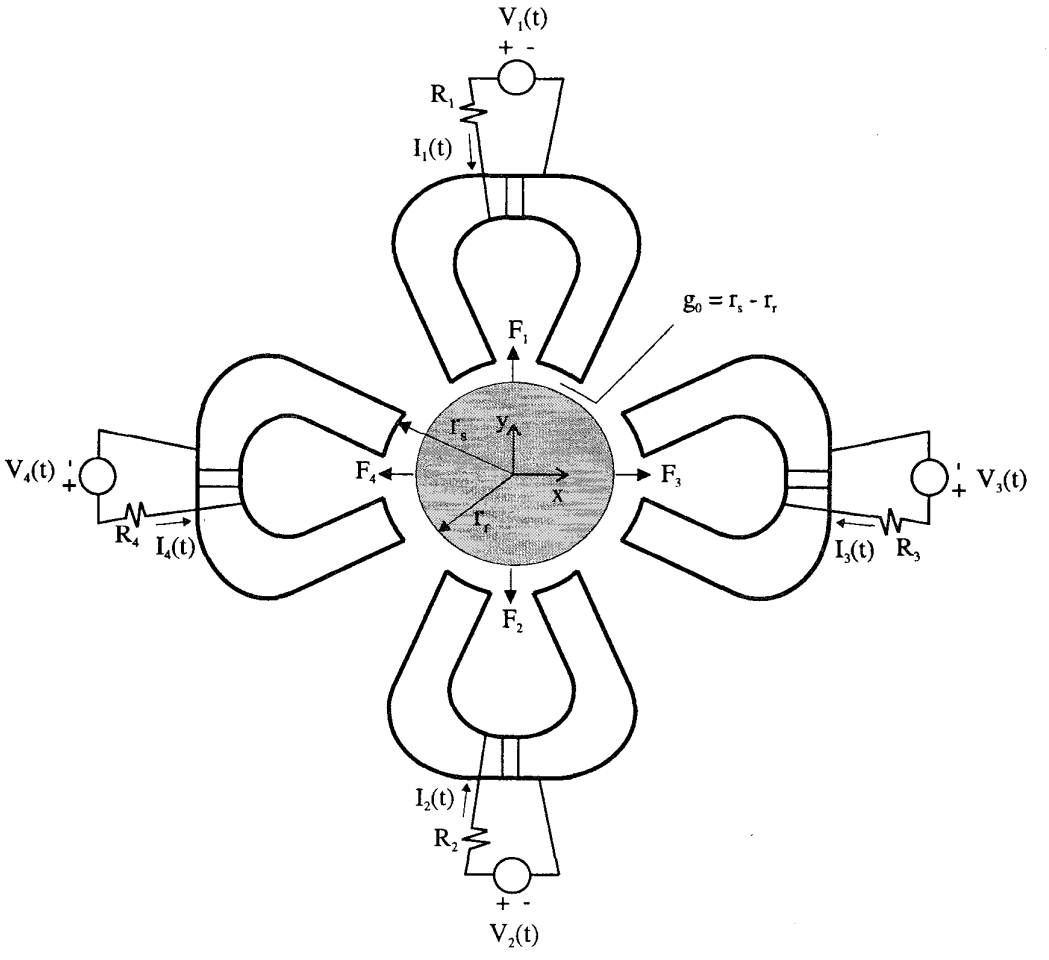

Fig. 1. Top view of a planar rotor disk magnetic bearing system.

subsystem (i.e., the desired current trajectory signals satisfy the static equation associated with the algebraic force transmission relationship).

This paper is organized as follows. In Section II, we present the electromechanical model and the modeling assumptions for the planar rotor disk AMB system. In Section III, we design the nonlinear controller and present the stability result. In Section IV, we illustrate how a specific flux linkage model can be utilized to explicitly design the desired current trajectory signals. To validate the performance of the proposed controller, we present some simulation results in Section V. Section VI concludes with some remarks.

II. Electromechanical Model

To facilitate the subsequent control development, we will assume that the mechanical subsystem model for the magnetic bearing system depicted by Fig. 1 [16] is given by

$$\begin{aligned} m\ddot{y} &= \sum_{i=1}^{2} F_i(y, I_i) \\ m\ddot{x} &= \sum_{j=3}^{4} F_j(x, I_j) \end{aligned} \tag{1}$$

where $y(t)$, $\dot{y}(t)$, and $\ddot{y}(t)$ represent the rotor disk position, velocity, and acceleration, respectively, along the y-direction (see Fig. 1), $x(t)$, $\dot{x}(t)$, and $\ddot{x}(t)$ represent the rotor position, velocity, and acceleration, respectively, along the x-direction, m represents the mass of the rotor, $F_i(y, I_i)$, $F_j(x, I_j)$ denote the forces produced by each stator electromagnetic circuit, and I_i, I_j represent the current in each stator coil. While the above definition for the magnetic forces is presented in very a general form, we have made the common simplifying assumption that the applied magnetic forces are only dependent on the direction of major motion and the measured current in winding of the coil (e.g., $F_1(y, I_1)$ only depends on y and I_1).

The flux linkage model allows us to compute the model for the force produced by the electrical phases as follows [19]:

$$\begin{aligned} F_i(y, I_i) &= \frac{\partial}{\partial y} \int_0^{I_i} \lambda_i(y, I_i)\, dI_i \\ F_j(x, I_j) &= \frac{\partial}{\partial x} \int_0^{I_j} \lambda_j(x, I_j)\, dI_j \end{aligned} \tag{2}$$

for $i = 1, 2$ and $j = 3, 4$, where $\lambda_i(y, I_i), \lambda_j(x, I_j)$ represent the flux linkage model. In addition, the flux linkage model allows us to compute the electrical subsystem dynamics for

the electrical phases as follows [19]:

$$\begin{aligned} L_i(y,I_i)\dot{I}_i + R_iI_i + B_i(y,I_i)\dot{y} &= v_i \\ L_j(x,I_j)\dot{I}_j + R_jI_j + B_j(x,I_j)\dot{x} &= v_j \end{aligned} \tag{3}$$

for $i = 1,2$ and $j = 3,4$, where v_i, v_j denotes the input voltage, R_i, R_j denotes the electrical resistance, and the inductance quantities $L_i(y,I_i), L_j(x,I_j)$ (which are assumed to be positive) and the back-EMF quantities $B_i(y,I_i), B_j(x,I_j)$ are calculated as follows [19]:

$$\begin{aligned} L_i(y,I_i) &= \frac{\partial \lambda_i(y,I_i)}{\partial I_i}, \qquad L_j(x,I_j) = \frac{\partial \lambda_j(x,I_j)}{\partial I_j} \\ B_i(y,I_i) &= \frac{\partial \lambda_i(y,I_i)}{\partial y}, \qquad B_j(x,I_j) = \frac{\partial \lambda_j(x,I_j)}{\partial x}. \end{aligned} \tag{4}$$

Remark 1: To facilitate the analysis, we require that $F_i(y,I_i)$, $F_j(x,I_j)$ be first-order differentiable and that $L_i(y,I_i)$, $L_j(x,I_j)$, $B_i(y,I_i)$, $B_j(x,I_j)$, $F_i(y,I_i)$, $F_j(x,I_j)$, $\partial F_i(y,I_i)/\partial I_i$, $\partial F_j(x,I_j)/\partial I_j$ are all bounded if x, y, I_i, I_j are bounded. For purposes of feedback and feedforward control, we will also assume that y, $\dot{y}$, I_i, x, $\dot{x}$, and I_j are measurable, and that the above electromechanical model is exactly known. We note that Hall effect sensors are usually utilized to measure the gap between the rotor and stator bearings (hence, y and x are measurable through the appropriate kinematic translations) while inexpensive current sensors can be used to measure I_i and I_j. To obtain $\dot{y}$ and $\dot{x}$, one might have to resort to numerically differentiating the position measurements, using model-based velocity observers, or using other nonlinear techniques [10].

III. Controller Development

Since the x and y directions are decoupled in the mechanical model defined in (1), we need only present the control strategy for the y-direction (i.e., the controller for the x-direction is a straightforward modification of the proposed controller). To facilitate the design of a rotor position tracking[2] controller for the electromechanical model given by (1) through (3), we define the rotor position tracking error and the corresponding filtered tracking error [15] as follows:

$$e = y_d - y \qquad r = \dot{e} + \alpha e \tag{5}$$

where $y_d(t)$ represents the desired rotor position trajectory in the y-direction, and α is a positive constant control gain (it is assumed that y_d, $\dot{y}_d$, $\ddot{y}_d$, $\dddot{y}_d$ are all bounded signals). To facilitate the subsequent control development, we also define the current tracking error (i.e., η_i) and the force tracking error (i.e., η_f) as follows:

$$\eta_i = I_{di} - I_i \qquad \eta_f = \sum_{i=1}^{2}[F_i(y,I_{di}) - F_i(y,I_i)] \tag{6}$$

where $I_{di}(t)$ represent the desired stator current trajectories for $i = 1,2$. The explicit definition for $I_{di}(t)$ will be given during the design procedure given below.

[2] Usually, the magnetic bearing problem is solved as a regulation problem; however, to provide increased flexibility (i.e., a "soft" desired position trajectory signal could be used when the bearing is initially energized), we will design a position tracking controller.

A. Mechanical Subsystem Design/Analysis

Given the definition of the filtered tracking error given in (5) and the force tracking error given by (6), we can write the mechanical subsystem dynamics of (1) as

$$m\dot{r} = m\ddot{y}_d + m\alpha\dot{e} - \sum_{i=1}^{2} F_i(y,I_{di}) + \eta_f \tag{7}$$

where the term $\sum_{i=1}^{2} F_i(y,I_{di})$ has been added to and subtracted from the right-hand side of (7). From the form of (7), we require that the desired current trajectory signals, denoted by $I_{di}(y,f_d)$, be designed to satisfy the following design equation:

$$\sum_{i=1}^{2} F_i(y,I_{di}) = f_d \tag{8}$$

where $f_d(t)$ denotes the desired force trajectory defined as follows:

$$f_d = m\ddot{y}_d + m\alpha\dot{e} + k_s r \tag{9}$$

with k_s being a positive control gain.

Remark 2: In addition to satisfying the relationship given by (8), the subsequent backstepping [8] procedure mandates the following design requirements on $I_{di}(y,f_d)$: 1) I_{di} must be bounded given that y, f_d are bounded, 2) I_{di} must be first-order differentiable, and 3) $\dot{I}_{di}$ must be bounded given that $y, \dot{y}, f_d, \dot{f}_d$ are bounded.

After explicitly substituting (8) and (9) into (7) and then simplifying the resulting expression, we obtain the closed-loop dynamics for the filtered tracking error in the following form:

$$m\dot{r} = -k_s r + \eta_f. \tag{10}$$

To provide motivation for a control term injected during the subsequent voltage control input design, we can perform the following preliminary analysis. Specifically, we define the nonnegative function

$$V_1 = \frac{1}{2}mr^2. \tag{11}$$

After taking the time derivative of (11) along (10), we can obtain the following expression:

$$\dot{V}_1 = -k_s r^2 + \eta_f r. \tag{12}$$

From the form of (12) and some knowledge of present nonlinear control techniques, we can see that the interconnection term (i.e., $\eta_f r$) prevents us from drawing conclusions regarding the regulation of the filtered tracking error; however, as we shall see in the next section, the effects of this term can be neutralized by injecting the appropriate terms into the current tracking error dynamics.

B. Electrical Subsystem Design/Analysis

To formulate the voltage control input, we take the time derivative of the current tracking error term defined in (6), and then substitute the electrical subsystem dynamics of (3) for $\dot{I}_i(t)$ to yield

$$\dot{\eta}_i = \frac{\partial I_{di}}{\partial f_d}\dot{f}_d + \frac{\partial I_{di}}{\partial y}\dot{y} + \frac{1}{L_i(y,I_i)}(R_i I_i + B_i(y,I_i)\dot{y} - v_i). \quad (13)$$

Given the definition of the desired force signal defined in (9), we can see that $f_d(t)$ can be expressed as a function of y, $\dot{y}$, and the desired motion trajectory; therefore, $\dot{f}_d(t)$ can be expressed as

$$\dot{f}_d = \frac{\partial f_d}{\partial \ddot{y}_d}\dddot{y}_d + \frac{\partial f_d}{\partial \dot{y}_d}\ddot{y}_d + \frac{\partial f_d}{\partial y_d}\dot{y}_d + \frac{\partial f_d}{\partial y}\dot{y} + \frac{\partial f_d}{\partial \dot{y}}\ddot{y} \quad (14)$$

where (9) can be used to compute the partial derivatives as follows:

$$\frac{\partial f_d}{\partial \ddot{y}_d} = m, \quad \frac{\partial f_d}{\partial \dot{y}_d} = m\alpha + k_s, \quad \frac{\partial f_d}{\partial y_d} = k_s\alpha$$
$$\frac{\partial f_d}{\partial y} = -k_s\alpha, \quad \frac{\partial f_d}{\partial \dot{y}} = -(m\alpha + k_s).$$

All of the quantities on the right-hand side of (14) are measurable except for $\ddot{y}$; however, from (1), the rotor acceleration can be written as

$$\ddot{y} = \frac{1}{m}\sum_{i=1}^{2} F_i(y, I_i). \quad (15)$$

After substituting (15) into (14), then substituting the resulting expression for $\dot{f}_d(t)$ into (13), we can write the open-loop current tracking dynamics for $\eta_i(t)$ in the following form:

$$\dot{\eta}_i = \Omega_i - \frac{v_i}{L_i(y,I_i)} \quad (16)$$

where $\Omega_i(t)$ is an auxiliary measurable function given by

$$\Omega_i = \frac{\partial I_{di}}{\partial f_d}\left(\frac{\partial f_d}{\partial \ddot{y}_d}\dddot{y}_d + \frac{\partial f_d}{\partial \dot{y}_d}\ddot{y}_d + \frac{\partial f_d}{\partial y_d}\dot{y}_d + \frac{\partial f_d}{\partial y}\dot{y} + \frac{\partial f_d}{\partial \dot{y}}\frac{1}{m}\sum_{i=1}^{2} F_i(y,I_i)\right) + \frac{\partial I_{di}}{\partial y}\dot{y} + \frac{1}{L_i(y,I_i)}(R_i I_i + B_i(y,I_i)\dot{y}). \quad (17)$$

Based on the open-loop dynamics of (16), the structure of (12), and the subsequent analysis, we define the voltage input control $v_i(t)$ as

$$v_i = L_i(y,I_i)(k_e\eta_i + \Omega_i + u_i) \quad (18)$$

where k_e is a positive control gain, and $u_i(t)$ is an auxiliary control input [17] utilized to sever the interconnections between the mechanical and electrical subsystem and is explicitly defined as follows:[3]

$$u_i = \begin{cases} \frac{F_i(y,I_{di}) - F_i(y,I_i)}{\eta_i} r & \text{if } \eta_i \neq 0 \\ \frac{\partial F_i(y,I_{di})}{\partial I_{di}} r & \text{if } \eta_i = 0. \end{cases} \quad (19)$$

[3]It is important to note that the definition of u_i when $\eta_i \neq 0$ reduces to the definition of u_i when $\eta_i = 0$ via L'Hospital's Rule. That is, the auxiliary control input u_i does not exhibit a singularity or a discontinuity.

After substituting the control input given by (18) into (16), we can write the closed-loop dynamics for $\eta_i(t)$ as follows:

$$\dot{\eta}_i = -k_e\eta_i - u_i. \quad (20)$$

To provide motivation for the design of the auxiliary control term defined in (19) while also preparing for the statement of the main result, we perform the following preliminary analysis. Specifically, we define the following nonnegative function:

$$V = V_1 + \frac{1}{2}\sum_{i=1}^{2}\eta_i^2 \quad (21)$$

where $V_1(t)$ was defined in (11). After taking the time-derivative of $V(t)$ defined by (21), and substituting (12) for $\dot{V}_1(t)$ and (20) for $\dot{\eta}_i(t)$, we can arrange $\dot{V}(t)$ in the following manner:

$$\dot{V} = -k_s r^2 - k_e\sum_{i=1}^{2}\eta_i^2 + \left[\eta_f r - \sum_{i=1}^{2}\eta_i u_i\right]. \quad (22)$$

If $\eta_i = 0$, then it is easy to see from the definition of $\eta_f(t)$ given in (6) that $\eta_f = 0$; hence, (22) becomes

$$\dot{V} = -k_s r^2 - k_e\sum_{i=1}^{2}\eta_i^2. \quad (23)$$

If $\eta_i \neq 0$, then we can substitute the definitions for $\eta_f(t)$ and $u_i(t)$ from (6) and (19), respectively, into the bracketed term in (22) to yield

$$\dot{V} = -k_s r^2 - k_e\sum_{i=1}^{2}\eta_i^2 + \left[r\sum_{i=1}^{2}(F_i(y,I_{di}) - F_i(y,I_i)) - r\sum_{i=1}^{2}\eta_i\left(\frac{F_i(y,I_{di}) - F_i(y,I_i)}{\eta_i}\right)\right] \quad (24)$$

which simplifies to the same result as that given by (23).

C. Composite Stability Result

Provided the design equation of (8) and the restrictions on $I_{di}(y,f_d)$ given in Remark 2 are satisfied, the proposed input voltage control ensures global exponential rotor position tracking. Specifically, we can use the form of (21) to state that $V(t)$ can be upper and lower bounded as follows:

$$\frac{1}{2}\lambda_1\|z\|^2 \leq V \leq \frac{1}{2}\lambda_2\|z\|^2 \quad (25)$$

where

$$z = [r, \quad \eta_1, \quad \eta_2]^T, \ \lambda_1 = \min\{m,1\}, \ \lambda_2 = \max\{m,1\}. \quad (26)$$

In addition, we can use the form of (23) to state that $\dot{V}$ can be upper bounded as follows:

$$\dot{V} \leq -\lambda_3\|z\|^2 \quad (27)$$

where

$$\lambda_3 = \min\{k_s, k_e\}.$$

From (25) and (27), standard Lyapunov type arguments [15] can be used to state that the filtered tracking error is exponentially stable in the following form:

$$\|r(t)\| \leq \|z(t)\| \leq \sqrt{\frac{\lambda_2}{\lambda_1}}\|z(0)\| \exp\left(\frac{-\lambda_3 t}{\lambda_2}\right).$$

Since the rotor position tracking error is related to the filtered tracking error according to the linear differential equation given by (5), we can use standard linear control arguments [15] to show that the rotor position tracking error is globally exponentially stable. From the above information and the structure of the voltage control input and the electromechanical system, we can also show that all of the system signals remain bounded during closed-loop operation.

Remark 3: The above control strategy suffers from two major drawbacks: 1) the controller requires exact model knowledge, and 2) the controller requires velocity measurements. To deal with uncertainty associated with any of the electromechanical parameters which appear linearly in the model, the above controller could be redesigned as an adaptive backstepping [8] controller to yield global asymptotic rotor position tracking. Under certain conditions on the structure of the electromechanical dynamics, the adaptive controller may also be further modified, as illustrated for multiphase electric machines in [18] and for the suspended ball problem in [10], to eliminate the requirement for velocity measurements.

Remark 4: In most of the previous work, a set of bearings is used to support a rotor shaft. That is, two of the magnetic bearing systems depicted in Fig. 1 are utilized to radially support a rigid vertical rotor [13] while an additional magnetic system can be used to regulate the shaft along the axial direction. In this setup, the control problem is complicated by the fact that the mechanical dynamics are coupled as opposed to the decoupled dynamics of (1). However, we can use standard techniques to derive the mechanical dynamics of the system as follows [7], [15]:

$$M(q)\ddot{q} + V_m(q,\dot{q})\dot{q} + G(q) = J^{-T}(q)\bar{F}(q, I_{ij}) \qquad (28)$$

where $q \in \Re^6$ is the rotor position vector, $M(q) \in \Re^{6\times 6}$ denotes the rotor inertia matrix, $V_m(q,\dot{q}) \in \Re^{6\times 6}$ represents the Coriolis-centripetal matrix, $G(q) \in \Re^6$ is the gravity vector, $J(q) \in \Re^{6\times 6}$ is a Jacobian matrix, and $\bar{F}(q, I_{ij}) \in \Re^6$ represents the transmitted force/torque vector defined as

$$\bar{F}(q, I_{ij}) = \left[\sum_{j=1}^{2} F_{1j}(q_1, I_{1j}),\ \sum_{j=1}^{2} F_{2j}(q_2, I_{2j}),\ \sum_{j=1}^{2} F_{3j}(q_3, I_{3j})\right.$$
$$\left.\sum_{j=1}^{2} F_{4j}(q_4, I_{4j}),\ \sum_{j=1}^{2} F_{5j}(q_5, I_{5j}),\ \tau_I - \tau_L\right]^T \in \Re^6$$

with q_i denoting the ith component of the position vector q, $F_{ij}(\cdot), I_{ij}(t)$ for $i = 1, \cdots, 5$ and $j = 1, 2$ denoting the forces and currents produced by each stator electromagnetic circuit, respectively, τ_I representing the input torque about the principal axis of the rotor shaft produced by a motor, and τ_L being the load torque about the principal axis of the shaft.

While the structure of the electromechanical system for the six degree-of-freedom (DOF) bearing system is substantially more complex that the dynamic equations given by (1) and (3), recent work in the design of nonlinear controllers for rigid-link electrically driven (RLED) robot manipulators illustrate that the problem is tractable. Specifically, adaptive full-state feedback and adaptive partial-state feedback controllers [3], [5] were recently designed for RLED manipulators actuated by multiphase electric machines. The form of (28) also illustrates that the input torque is mechanically coupled to the forces applied by the magnetic bearing system; hence, it seems that the magnetic bearing control system and the control system which generates the input torque must be designed in tandem to accurately control the position of the shaft.

IV. Desired Current Trajectory Design Example

If fringing and leakage are neglected and the magnetic circuit is assumed to be linear, the following flux linkage model is often utilized to complete the electromechanical dynamic system description of Section II [16]:

$$\lambda_i(y, I_i) = L_i(y) I_i \qquad \lambda_j(x, I_j) = L_j(x) I_j \qquad (29)$$

where

$$L_i(y) = \frac{L_0}{2(g_o + (-1)^i y) + L_1}$$
$$L_j(x) = \frac{L_0}{2(g_o + (-1)^j x) + L_1} \qquad (30)$$

L_0, L_1 are positive constant parameters which depend on the number of stator coil turns, permeability of the material/air, cross-sectional area of the electromagnet, etc., and g_o is a constant kinematic quantity given by $g_o = r_s - r_r$ (see Fig. 1). The flux linkage model given by (29) can now be used to calculate the quantities given by (2) and (4). For example, $F_i(y, I_i)$ of (2) is explicitly given by

$$F_i(y, I_i) = \frac{(-1)^{i+1} L_0 I_i^2}{(2(g_o + (-1)^i y) + L_1)^2}. \qquad (31)$$

Note that by substituting (31) into (19), the expression for u_i simplifies to

$$u_i = \frac{(-1)^{i+1} L_0}{(2(g_o + (-1)^i y) + L_1)^2}(I_{di} + I_i) r. \qquad (32)$$

We now illustrate how the flux linkage model given by (29) can be used to design the desired current trajectories such that the design equation given by (8) and the restrictions on $I_{di}(y, f_d)$ given in Remark 2 are satisfied. Specifically, after substituting (31) into (8), we must construct $I_{di}(y, f_d)$ to satisfy

$$\sum_{i=1}^{2} \frac{(-1)^{i+1} L_0 I_{di}^2}{(2(g_o + (-1)^i y) + L_1)^2} = f_d. \qquad (33)$$

To satisfy (33), we first design $I_{di}(t)$ to cancel some of the terms as follows:

$$I_{di} = \frac{1}{\sqrt{L_0}}(2(g_o + (-1)^i y) + L_1)\sqrt{\gamma_{di}} \qquad (34)$$

where $\gamma_{di}(f_d)$ is an auxiliary function which must be designed to be nonnegative to ensure that (34) is well posed. After substituting the right-hand side of (34) into (33) for I_{di}, we must now design $\gamma_{di}(f_d)$ to satisfy the following relationship:

$$\sum_{i=1}^{2}(-1)^{i+1}\gamma_{di} = f_d. \tag{35}$$

Based on the structure of (35) and the backstepping constraints discussed in Remark 2, we now design the auxiliary function $\gamma_{di}(f_d)$ as follows:[4]

$$\gamma_{di} = \frac{1}{2}\left((-1)^{i+1}f_d + \sqrt{f_d^2+\gamma_0^2}\right) \tag{36}$$

where the positive scalar design parameter γ_0 is used to set the desired threshold winding current.

To illustrate the motivation for the structure of (36), we substitute (36) into (35) to yield

$$\sum_{i=1}^{2}(-1)^{i+1}\left(\frac{1}{2}\left((-1)^{i+1}f_d + \sqrt{f_d^2+\gamma_0^2}\right)\right) = f_d \tag{37}$$

which can be rewritten as

$$\frac{1}{2}f_d + \frac{1}{2}\sqrt{f_d^2+\gamma_0^2} + \frac{1}{2}f_d - \frac{1}{2}\sqrt{f_d^2+\gamma_0^2} = f_d. \tag{38}$$

Hence, we can now see from (38) that $I_{di}(y, f_d)$ has been designed to ensure that desired force trajectory is delivered to the mechanical subsystem. That is, the desired current trajectory of (34) and (36) has been designed to satisfy the relationship given by (8).

Remark 5: It is important to note that the physical geometry of the mechanical system (see Fig. 1) ensures that $|y(t)| \leq g_o = r_s - r_r$; hence, if $\gamma_{di}(t) \geq 0$, then $I_{di}(t) \geq 0$ for all time. It is also easy to see from (36) that

$$\lim_{f_d \to 0}\gamma_{di} = \frac{1}{2}\gamma_0. \tag{39}$$

Given the form of (34) and (36), we can now state that γ_{di}, I_{di} are bounded given that y, f_d are bounded (i.e., Condition 1) in Remark 2 has been satisfied).

Remark 6: During the formulation of the current tracking error dynamics, we required the calculation of two partial derivative terms associated with $I_{di}(y, f_d)$ [i.e., $\partial I_{di}/\partial f_d$ and $\partial I_{di}/\partial y$ in (13)]. Based on (34) and (36), these partial derivative terms can now be calculated as follows:

$$\frac{\partial I_{di}}{\partial f_d} = \frac{2(g_o+(-1)^i y)+L_1}{4\sqrt{\gamma_{di}L_0}}\left((-1)^{i+1} + \frac{f_d}{\sqrt{f_d^2+\gamma_0^2}}\right) \tag{40}$$

and

$$\frac{\partial I_{di}}{\partial y} = 2(-1)^i\sqrt{\frac{\gamma_{di}}{L_0}} + \frac{1}{4\sqrt{\gamma_{di}L_0}}(2(g_o+(-1)^i y)+L_1) \times \frac{\partial f_d}{\partial y}\left((-1)^{i+1} + \frac{f_d}{\sqrt{f_d^2+\gamma_0^2}}\right). \tag{41}$$

[4] Since the equality given by (35) and the backstepping constraints given in Remark 2 are somewhat unrelated, we employed some tedious guess work during the formulation of (36).

Hence, the desired current trajectory signal has been constructed such that the above partial derivatives can be calculated; therefore, Condition 2) in Remark 2 is satisfied. We can also use the composite stability result and the structure of (40) and (41) to state that $\dot{I}_{di}$ is bounded given that y, $\dot{y}$, f_d, and $\dot{f}_d$ are bounded (i.e., Condition 3) in Remark 2 is satisfied). Indeed, from the structure of $\partial I_{di}/\partial f_d$ and $\partial I_{di}/\partial y$, we can now see the reason for including the desired threshold winding current design parameter γ_0 during the construction of (36) (i.e., as a result of (39), we can see that the use of γ_0 ensures that the partial derivatives of $I_{di}(t)$ do not blow up as $f_d \to 0$).

V. Simulation

The controller described in Sections III and IV was simulated for the planar rotor disk AMB system of Fig. 1. The applied control law can be summarized as follows:

$$\begin{cases} \text{voltage input: } v_i = L_i(y, I_i)(k_e\eta_i + \Omega_i + u_i) \\ \text{desired current: } I_{di} = \frac{1}{\sqrt{L_0}}(2(g_o+(-1)^i y)+L_1) \cdot \sqrt{\frac{1}{2}\left((-1)^{i+1}f_d + \sqrt{f_d^2+\gamma_0^2}\right)} \\ \text{desired force: } f_d = m\ddot{y}_d + m\alpha\dot{e} + k_s r \end{cases}$$

where $L_i(y, I_i)$, η_i, Ω_i, u_i, and r were defined in (30), (6), (17), (32), and (5), respectively. The system parameters utilized in the simulation were

$$m = 2.0 \text{ kg}, \quad g_o = 10^{-3} \text{ m}, \quad L_0 = 3.0 \times 10^{-4} \text{ H·m}$$
$$L_1 = 1.25 \times 10^{-5} \text{ m}, \quad R_1 = R_2 = R_3 = R_4 = 1.0\ \Omega. \tag{42}$$

Although the controller was designed to solve the tracking problem, the simulation was performed to regulate the planar rotor disk; hence, the desired position trajectory in the y-direction was chosen as

$$y_d(t) = 0.5e^{-t} \times 10^{-3} \text{ m}.$$

The initial position of the center of the rotor disk on the y axis was set to $y(0) = -0.2 \times 10^{-3}$ m while the initial velocity and electrical currents were set to zero.

First, the simulation was performed assuming exact knowledge of the parameter values given in (42). The set of control gains and the design parameter γ_0 that resulted in good tracking performance were as follows:

$$\alpha = 2.0, \quad k_s = 5.0, \quad k_e = 10.0, \quad \gamma_0 = 0.6. \tag{43}$$

Fig. 2 illustrates the position tracking error in the y-direction, the input voltages v_1, v_2, and the stator currents I_1, I_2. The same results can be obtained for the x-direction. We observed that increasing the control gain α the tracking error had a faster decay while changes in k_s, k_e, and γ_0 had little influence in the system response. Next, the controller robustness was evaluated by considering a 25% uncertainty in the parameter values given in (42) (except for g_o). The control gains and γ_0 were set to the same values as given in (43). Fig. 3 illustrates the system performance. For this case, it was observed that the use of larger values for γ_0 degraded substantially the tracking performance even causing instability.

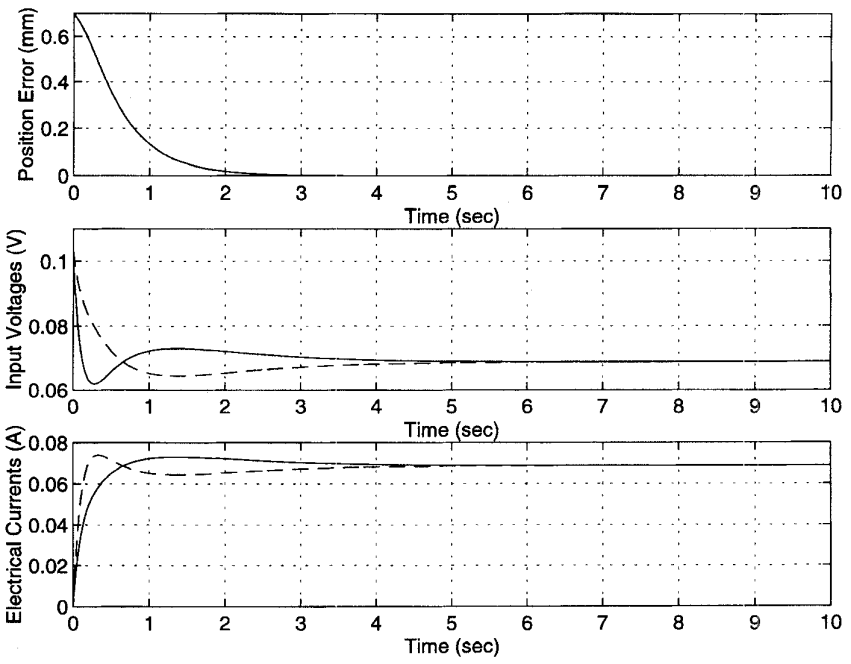

Fig. 2. System performance with exact parameter knowledge.

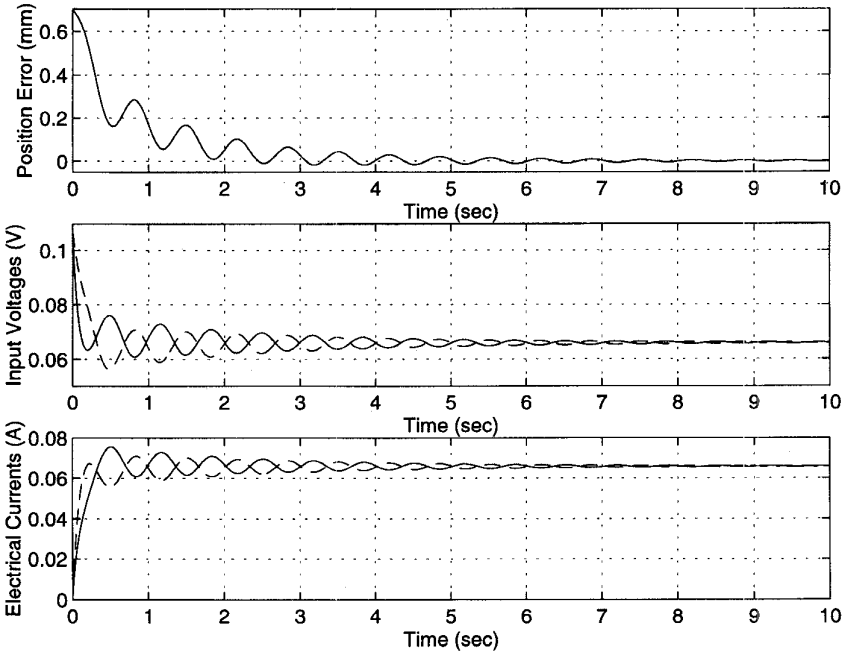

Fig. 3. System performance with parametric uncertainty.

VI. Conclusion

In this paper, we have illustrated how the integrator backstepping control design tools can be utilized to design a controller for the nonlinear dynamic equations representing a planar rotor disk, magnetic bearing system which depends on a general flux linkage model. Provided the desired current trajectory signals can be constructed to deliver the desired force to the mechanical subsystem by satisfying a static design equation while also satisfying some mild constraints imposed by the backstepping procedure, the controller yields global exponential position tracking. An example flux linkage model was then used to illustrate how the desired current trajectory signals can be constructed, and hence, complete the control description. Remarks on the possible extensions

of the proposed control structure, such as compensating for parametric uncertainty, eliminating state measurements, and upgrading to the six-DOF model, were also discussed.

Since the controller has been developed for a general flux linkage model, it may be possible to redesign the desired current trajectory signals for a more sophisticated flux linkage model than the one used in (29). That is, the flux linkage model for each electromagnetic circuit should probably include dependencies on both position directions and all of the electrical currents [e.g., $\lambda_i(x, y, I_1, I_2, I_3, I_4)$], as well as exhibit an improved functional form which accounts for the shape of the rotor and the stator [4]. While it is possible to revise the design procedure to account for the new coupling in the electrical subsystem dynamics (i.e., assuming the composite inductance matrix is positive definite), it is unclear whether the new algebraic force transmission relationships would greatly hinder the construction of *suitable* desired current trajectory signals which ensure that the desired force is delivered to the mechanical subsystem and satisfy the conditions in Remark 2.

REFERENCES

[1] S. Beale, B. Shafai, P. LaRocca, and E. Cusson, "Adaptive forced balancing for magnetic bearing control system," in *Proc. IEEE Conf. Decision and Control*, Tucson, AZ, Dec. 1992, pp. 3535–3539.

[2] H. Bleuler, D. Vischer, G. Schweitzer, A. Traxler, and D. Zlatnik, "New concepts for cost-effective magnetic bearing control," *Automatica*, vol. 30, no. 5, pp. 871–876, May 1994.

[3] M. M. Bridges and D. M. Dawson, "Adaptive control for a class of direct drive robot manipulators," in *Proc. 4th Wkshp. on Nonlinear Adaptive Contr.: Applications to Nonlinear Syst. and Robot.*, Cancun, Mexico, Dec. 1994.

[4] W. Brzezina and J. Langerholc, "Lift and side forces on rectangular pole pieces in two dimensions," *J. Appl. Phys.*, vol. 45, no. 4, pp. 1869–1872, Apr. 1974.

[5] T. Burg, D. Dawson, J. Hu, and S. Lim, "An adaptive partial state feedback controller for RLED robot manipulators actuated by BLDC motors," in *Proc. IEEE Conf. Robotics Automation*, Nagoya, Japan, May 1995, pp. 300–305.

[6] A. Charara, B. Caron, and G. Lemarquand, "Modeling and noninteractive control of an active magnetic bearing," *J. Appl. Electromagn. Materials*, vol. 2, no. 3–4, 1991.

[7] B. Etkin, *Dynamics of Flight—Stability and Control*. New York: Wiley, 1959.

[8] P. Kokotovic, "The joy of feedback: Nonlinear and adaptive," *IEEE Contr. Syst. Mag.*, vol. 12, pp. 177–185, June 1992.

[9] P. Krause, *Analysis of Electric Machinery*. New York: McGraw-Hill, 1986.

[10] M. Krstic, I. Kanellakopoulos, and P. Kokotovic, *Nonlinear and Adaptive Control Design*. New York: Wiley, 1995.

[11] F. Matsumura and T. Yoshimoto, "System modeling and control design of a horizontal-shaft magnetic-bearing system," *IEEE Trans. Magn.*, vol. MAG-22, May 1986.

[12] A. M. Mohamed and F. P. Emad, "Conical magnetic bearings with radial and thrust control," *IEEE Trans. Automat. Contr.*, vol. 37, pp. 1859–1868, Dec. 1992.

[13] A. M. Mohamed and I. Busch-Vishniac, "Imbalance compensation and automatic balancing in magnetic bearing systems using the Q-parameterization theory," in *Proc. Amer. Contr. Conf.*, Baltimore, MD, June 1994, pp. 2952–2957.

[14] S. Sastry and M. Bodson, *Adaptive Control: Stability, Convergence, and Robustness*. Englewood Cliffs, NJ: Prentice-Hall, 1989.

[15] J. Slotine and W. Li, *Applied Nonlinear Control*. Englewood Cliffs, NJ: Prentice-Hall, 1991.

[16] R. D. Smith and W. F. Weldon, "Nonlinear control of a rigid rotor magnetic bearing system: Modeling and simulation with full state feedback," *IEEE Trans. Magn.*, vol. 31, pp. 973–980, Mar. 1995.

[17] E. Sontag and H. Sussman, "Further comments on the stabilization of the angular velocity of a rigid body," *Syst. Contr. Lett.*, vol. 12, pp. 213–217, 1988.

[18] P. Vedagarbha, T. Burg, J. Hu, and D. Dawson, "Development and demonstration of new class of adaptive partial state feedback controllers for electric machines," in *Proc. Amer. Contr. Conf.*, June 1995, pp. 59–63.

[19] H. H. Woodson and J. R. Melcher, *Electromechanical Dynamics—Part I: Discrete Systems*. New York: Wiley, 1968.

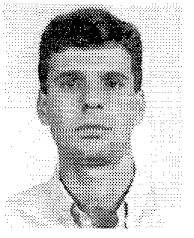

Marcio S. de Queiroz was born in Rio de Janeiro, Brazil in 1966. He received the B.S. degree in electrical engineering from the Federal University of Rio de Janeiro, Brazil, in 1990 and the M.S. degree in mechanical engineering from the Pontifical Catholic University of Rio de Janeiro, Brazil, in 1993. He is currently a Ph.D. student in the Department of Electrical and Computer Engineering at Clemson University, Clemson, SC.

His research interests are in application of nonlinear control to electromechanical systems.

Darren M. Dawson (S'89–M'90–SM'94) was born in 1962 in Macon, GA. He received the Associate Degree in mathematics from Macon Junior College, Macon, GA, in 1982 and the B.S. degree in electrical engineering from the Georgia Institute of Technology, Atlanta, in 1984. In 1987, he returned to the Georgia Institute of Technology where he received the Ph.D. degree in electrical engineering in March 1990.

He worked for Westinghouse as a Control Engineer from 1985 to 1987. During his Ph.D. studies, he also served as a Research/Teaching Assistant. In July 1990, he joined the Electrical and Computer Engineering Department and the Center for Advanced Manufacturing (CAM) at Clemson University, Clemson, SC, where he currently holds the position of Professor. Under the CAM Director's supervision, he currently leads the Robotics and Manufacturing Automation Laboratory which is jointly operated by the Electrical and Mechanical Engineering Departments. His main research interests are in the fields of nonlinear based robust, adaptive, and learning control with application to electromechanical systems including robot manipulators, motor drives, magnetic bearings, rapid isothermal processing, and distributed systems.